NASw-54

37

UNPUBLISHED PRELIMINARY DATA

[redacted]

Cosmic Radio Intensities at 1.225 and 2.0 Megacycles/sec Measured up to an Altitude of 1700 Kilometers

GPO PRICE $ _____

OTS PRICE(S) $ _____

Hard copy (HC) 2.00

Microfiche (MF) .50

D. Walsh, F. T. Haddock, and H. F. Schulte
Radio Astronomy Observatory
The University of Michigan
Ann Arbor, Michigan

For the COSPAR 6th Plenary meeting and 4th International Space Science Symposium, Warsaw, Poland, June, 1963

[redacted]

Abstract

"Cosmic Radio Intensities at 1.225 and 2.0 Megacycles/sec Measured up to an Altitude of 1700 Kilometers"

D. Walsh, F. T. Haddock, and H. F. Schulte

14390

A description is given of a rocket flight to 1700 km altitude for the purpose of measuring cosmic noise intensities at 0.75, 1.225 and 2.0 Mc. Above the peak of the ionosphere no signals originating on the bottomside were detected.

Modulation of the radiometer outputs due to vehicle spin was observed throughout the trajectory. At the higher parts this was unrelated to the ionosphere and was presumably due to non-uniformity of sky brightness. At lower altitudes a series of ionospheric effects was observed and is discussed in relation to impedance behavior of an antenna in a magneto-ionic plasma.

The disappearance of the extraordinary wave at the level $X = 1 - Y$ was detected and clearly identified by the sharp drop in signal and the enhanced angle-dependence of the radiation resistance. Previously unreported regions in the ionosphere of high noise levels were detected, and the conditions for their occurrence in relation to propagation behavior in the ionosphere is delineated.

The validity of semi-theoretical corrections of cosmic noise measurements for the plasma influence on the antenna is demonstrated. Cosmic noise intensities at 1.225 and 2.0 Mc of 1.0×10^{-20} and 2.0×10^{-20} W m^{-2} $(c/s)^{-1}$ sr^{-1} respectively were obtained. Combined with selected higher frequency measurements this shows a sharp break in the spectrum near 2.0 Mc.

The corresponding cosmic brightness temperatures are 2.1×10^{7}° K and 1.7×10^{7}°K, at 1.225 and 2.0 Mc, respectively.

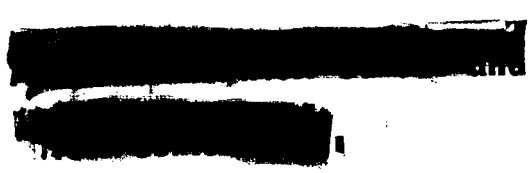

"Cosmic Radio Intensities at 1.225 and 2.0 Megacycles/sec Measured up to an Altitude of 1700 Kilometers"

D. Walsh, F. T. Haddock, and H. F. Schulte
Radio Astronomy Observatory
The University of Michigan
Ann Arbor, Michigan

1. Introduction

The scientific possibilities and importance of using rockets and satellites to conduct radio astronomy observations at low frequencies has been recognized for several years[1-4]. Radio astronomy observations below 10 Mc from the ground were carried out a number of years ago but were complicated by ionospheric effects. The pioneering measurements by Reber and Ellis in 1955 [5] pointed out the possibilities of radio astronomy measurements from the ground at frequencies down to 1 Mc. Ellis and his associates have continued this work which includes measurements of the cosmic noise background level at frequencies between 1 and 10 Mc [6,7]. However, uncertainties in the calibration of the antenna efficiency, ionospheric absorption, refraction and scattering effects are involved. Therefore it is important to conduct similar measurements from rockets and satellites at the same frequencies and lower.

The only reported space radio astronomy measurements at low frequencies have been by the Ottawa group who obtained measurements of the cosmic noise background at 3.8 Mc from a satellite with apogee at 1070 km [8,9]. These measurements were discussed by Chapman and Molozzi [10,11] who deduced a value for the average sky brightness temperature at this frequency of 8.1×10^6 °K. Smith [12] independently discussed the Ottawa observations and derived from them a mean brightness temperature of 1.3×10^6 °K for a comparable area of sky. This discrepancy of a factor six is apparently due to differences of interpretation of the effects of local plasma on the system sensitivity. No in-flight measurements of such effects were made so Chapman and Molozzi had to resort to rather indirect methods of analysis to account for them.

In 1959 the University of Michigan Radio Astronomy Observatory commenced the design of a rocket experiment to measure the mean cosmic noise background at low frequencies. The design of the system arose from the conviction that in-flight calibration of the antenna and receiver characteristics would be essential for the interpretation of both the expected and any unexpected effects. It would also give the measured cosmic noise intensities sufficient accuracy to be of scientific value. It was felt desirable to make measurements at a range of frequencies to help interpret ionospheric effects, and hopefully to define the cosmic noise spectrum. Several spot-frequency receivers rather than a sweep-frequency receiver were chosen because ground experience had suggested that these would be easier to calibrate to obtain accurate absolute values. The choice of frequencies of 0.75, 1.225 and 2.0 Mc was determined by expected vehicle performance and the rather scant data available at the time on the topside of the ionosphere. For practical purposes, an electrically short dipole was chosen rather than a magnetic loop. The payload resulting from this design was launched on 22 September 1962, and both the rocket and payload performed well. An altitude of almost 1700 km was reached.

For proper interpretation of the data an understanding of the antenna behavior in the plasma is essential. Consequently, several important features of this subject will be discussed. A number of authors have discussed the subject of ionospheric focusing [11,13-15] . Thus it will not be enlarged upon here, except to say that at apogee it is believed from ray-tracing calculations that the antenna beam at both 1.225 and 2.0 Mc covered essentially the whole of the upper hemisphere of sky. The equipment and the observations obtained will then be discussed and the interpretation of the data, involving the derivation of the topside ionospheric profile and a number of previously unreported phenomena, will be given. Cosmic noise intensities at 1.225 and 2.0 Mc will be deduced, and a comparison with selected work at these and higher frequencies will be made. Finally, the astronomical implications of these measurements will be discussed.

2. Antenna behavior in a plasma

2.1 Equivalent circuit

When an antenna is receiving noise power, there is in any frequency range $\Delta\nu$ a limited available power P_A which can be drawn, and it is usual to define an average antenna temperature for the range $\Delta\nu$ by $P_A = kT_A\Delta\nu$, k being Boltzmann's constant. The antenna temperature at a particular frequency is obtained by taking the limit as $\Delta\nu$ goes to zero. If the incident radiation from direction (θ,ϕ) has brightness temperature $T_B(\theta,\phi)$ and the antenna has gain $g(\theta,\phi)$ in that direction, then it is well known that

$$T_A = \frac{1}{4\pi}\int_{4\pi} g(\theta,\phi)T_B(\theta,\phi)d\Omega \qquad (2.1)$$

where the integral is taken over the whole solid angle, or $T_A = \langle T_B \rangle$ where $\langle T_B \rangle$ means an average of $T_B(\theta,\phi)$ weighted by the antenna gain distribution. If T_B is the same for all directions than $T_A = T_B$. Caution must be taken in using the preceding concepts and definitions if the incident radiation is not randomly polarized.

At any particular frequency it is convenient to introduce a Thevenin equivalent circuit with open circuit voltage V_A, series resistance R_A and reactance X_A. In fig. 1 the reactance is shown as a capacitance since this will be the case in most of the remaining discussion. It will be assumed that there are no losses, so R_A is the radiation resistance, and $P_A = V_A^2/4R_A$ so that

$$V_A^2 = 4kT_AR_A\Delta\nu. \qquad (2.2)$$

In practice, the quantity actually measured is the voltage V_L at the receiver input terminals. The receiver in fig. 1 is represented by its input impedance $Z_L = R_L + jX_L$ which is, in general, frequency dependent and includes any base capacity inherent in the mounting of the antenna. In order to relate V_L to the desired quantity T_A it is necessary to know R_A and C_A; this is true whether or not an attempt is made to use a matched system.

For an electrically short dipole in a uniform plasma without a superposed magnetic field, it is readily shown that $R_A = nR_{Ao}$ and $C_A = n^2 C_{Ao}$ where suffixes zero indicate free-space values and $n^2 = 1 - X$, X being the usual magneto-ionic parameter (plasma frequency/wave frequency)^2.

A plasma with a superposed static magnetic field is doubly refracting and the radiation resistance must be divided into two additive components R_I and R_{II} corresponding to the two characteristic waves which propagate, as discussed in section 2.2. Each must have its own temperature associated with it. Thus by an extension of eq. (2.1)

$$T_I = \frac{1}{4\pi} \int_{4\pi} g_I(\theta,\phi) T_{BI}(\theta,\phi) d\Omega \qquad (2.3)$$

with a similar expression for T_{II}. The gain distributions g_I and g_{II} may be quite different; the incident radiation in the characteristic waves may not be randomly polarized; and T_{BI} may be quite different from T_{BII}. Thus, in general, T_I and T_{II} will not be the same.

R_I and R_{II} each have an equivalent generator associated with them in the manner of eq. (2.2) so that

$$V_A^2 = 4k(T_I R_I + T_{II} R_{II})\Delta\nu \qquad (2.4)$$

and

$$T_A = \frac{T_I R_I + T_{II} R_{II}}{R_I + R_{II}} \qquad (2.5)$$

T_A is, then, an average of T_I and T_{II} weighted by their respective radiation resistances. In the particular case where the antenna beam is completely filled with a source of uniform brightness temperature T_B, then $T_A = T_I = T_{II} = T_B$, independent of antenna impedance.

2.2 Radiation resistance

Kogelnik [16] has derived an integral expression for the radiation resistance of an elementary electric dipole in a magneto-ionic medium. His result has been discussed by Weil and Walsh [17] who show that it may be separated into two components R_I and R_{II} associated with the respective characteristic waves, and who give extensive numerical results.

The convention adopted is that the label I is applied to that characteristic wave which is independent of the strength of the magnetic field when propagating perpendicularly to it. This is widely called the ordinary wave.

It is instructive to consider fig. 2, which is often useful in plasma physics. The ordinate Y^2 employs the magneto-ionic parameter Y = (gyro-frequency/wave frequency). The origin represents free-space conditions; and radiation entering the outer ionosphere starts there and traces a trajectory on the diagram as it penetrates into the plasma. The behavior of the refractive index has been examined in considerable detail by, for example, Ratcliffe [18]. Thus both characteristic waves propagate in region 1, but the wave II cannot cross into region 2. Wave I can propagate through regions 1, 2, 3 and 6, but cannot cross line X = 1.

In region 3 (cross-hatched) wave II can propagate, and in regions 7 and 8 (also cross-hatched) wave I can propagate, but in each case the refractive index becomes infinite for some direction relative to the magnetic field. This causes Kogelnik's integral expression to become infinite; however, infinite refractive index implies zero wave length so that no real antenna could be considered electrically short, and consequently the application of his theory to a real antenna would be invalid. It appears that the behavior of radiation resistance in these regions is inadequately understood at present; presumably it requires more detailed consideration of the current distribution which cannot be assumed to be the simple one used for an electrically short dipole.

From the work of Weil and Walsh, typical curves applicable to a wave frequency of 1.225 Mc are reproduced in fig. 3. The radiation resistance relative to its free-space value may be written

$$R_A/R_{Ao} = M + N \cos^2\psi \qquad (2.6)$$

where ψ is the angle between the dipole and the magnetic field. M and N may be split into components M_I, M_{II}, N_I, N_{II}, but only the sums are shown. It will be noted that at a fixed gyro-frequency, as the plasma frequency is increased, M decreases steadily at first, then plunges rather rapidly to a cusp, after which it decreases relatively slowly again. Similarly, N is extremely small at first, then rises sharply as M plunges, also reaching a cusp, and then flattening. The cusp corres-

ponds to the non-propagation of characteristic wave II and disappearance of M_{II} and N_{II} beyond $X = 1 - Y$. At frequencies well below this the small value of N indicates little variation of R_A with angle, but the variation builds up rapidly as the cusp is approached.

2.3 Capacitance

Although a variety of expressions has appeared in the literature, an exact expression for the capacitance of a cylindrical dipole in free space cannot be obtained. Kaiser [19] has derived an approximate expression for the capacitance of an electrically short biconical antenna in a magneto-ionic medium, neglecting radiation resistance. His result for C_A/C_{Ao}, the ratio of the capacitance in free space to its value in the medium, again neglecting collisions, becomes $(1 - X)$ for the case of zero magnetic field, as would be expected. Referring to fig. 2, his result leads to a capacitance equal to zero on the lines $X = 1 - Y^2$ and $X = 1$, $+\infty$ on the line $Y = 1$ for $X < 1$, and $-\infty$ on the line $Y = 1$ for $X > 1$. In regions 1 and 2 and also 6, C_A is positive, and in regions 4 and 5 it is negative, i.e., inductive.

Kaiser deduces that in regions 3, 7 and 8 the capacitance becomes complex, that is, it has a loss term associated with it even in the absence of collisions. However, it seems likely that his treatment is inapplicable in these regions for the same reason that the radiation resistance theory breaks down; namely that the infinity in the refractive index of one or another characteristic wave invalidates the assumption of an electrically short antenna. In any case, Kaiser's neglect of radiation resistance is apparently unjustified in these regions since, as pointed out in section 2.2, it may become infinite. It is possible that the theories for both radiation resistance and capacitance do not break down suddenly at the boundaries of these regions, but rather become progressively less accurate as the boundaries are approached.

In practice, an ion sheath will form around the antenna due to the vehicle acquiring a negative potential relative to the plasma. Kaiser [19] and Kane, Jackson and Whale [20] suggest that this may be taken into account approximately by considering the capacity between the two halves

of the antenna to be a series combination of the capacitance between the antenna and sheath boundary, with unity dielectric constant, and the capacitance within the medium. The latter may be considered to be the capacitance of a dipole with radius equal to that of the sheath dimension.

2.4 Summary

Suppose a receiving system using a short electric dipole starts from a great height where conditions are essentially free space and decends into the topside of the ionosphere, so that both the plasma frequency and the gyro-frequency increase, tracing out a trajectory starting at the origin of fig. 2. In general, the antenna temperature will vary as the gain distribution over the non-uniformly bright sky changes, but this effect will usually be small compared with those produced by the impedance changes. Thus in fig. 1, the antenna series reactance will increase, both effects will cause the voltage V_L to decrease, and the receiver output will decrease accordingly. The decrease would be expected to be rather abrupt as the boundary between region 1 and region 2 is approached and characteristic wave II, generally called the extraordinary wave in region 1, ceases to propagate and R_{II} becomes zero. In region 2 the rate of decrease should at first be less rapid as R_I decreases smoothly; but according to Kaiser's analysis C_A should drop to zero at the boundary between regions 2 and 3 so that the voltage at the receiver terminals would be zero. In region 3 the antenna behavior is very uncertain, but wave I, the ordinary wave, can propagate and presumably would be received. If the trajectory passes into region 4, then wave II can propagate but cannot cross into region 4 from the origin through the barrier of region 2. Thus no wave from outside the atmosphere should be received. On the other hand if the trajectory passes from region 3 into region 6, where the impedance is well-behaved, wave I should still be received with decreasing receiver output until the trajectory crosses the line $X = 1$.

3. Description of equipment

The payload system is shown in simplified form in fig. 4. The radio astronomy antenna is an electrically short, balanced dipole which is arranged to deploy after rocket nose cone ejection at an altitude of 700 km. The fully deployed antenna length is 12.32 m, tip to tip.

A balanced switching system periodically connects this antenna first to the wide-band, preamplifier input and then to the antenna capacitance measuring circuit. While the switch is in the C_A measurement position, the preamplifier is connected to a balanced dummy antenna which matches the free-space electrical characteristics of the radio astronomy antenna. It is designed to allow the introduction of a known amount of calibration signal from the noise generator. Details of the 12-second repetitive switching sequence are presented in table 1.

In addition to the above, the in-flight telemetering system is calibrated separately every sixth complete cycle.

The wide-band, low-noise preamplifier employs vacuum tubes and has a bandpass from 0.7 to 2.2 Mc. The preamp gain over this band is large enough to establish the signal-to-noise ratio for each radiometer channel at the preamp input. No attempt was made to tune out the antenna capacitance since this would lead to excessive changes in the system response due to the ionospheric effects. Three identical output drivers simultaneously feed conventional superheterodyne receivers operating at 0.75, 1.225 and 2.0 Mc. The receiver bandwidth at the second detector is 3.4 kc. The detector output is passed through a simple low-pass RC time averaging network with a charge and discharge time constant of 0.1 second. After additional signal conditioning, the outputs are fed to separate subcarrier channels of a standard FM/FM telemetering system operating at 240 Mc. The 9-watt telemetering transmitter drives a phased turnstile antenna.

Provision is made to telemeter the unsmoothed audio output of each radiometer channel. Each channel is sampled for 12 seconds in sequence. Aural and oscillographic monitoring of each channel provides the capability of detecting man-made or atmospheric leakage from the ground or spurious receiver oscillations.

Two additional telemetering subcarrier channels are utilized; one carries acceleration data for vehicle performance evaluation, and the second is time-multiplexed with a 30-channel commutator to monitor equipment temperatures, voltage levels, vehicle aspect and antenna deployment and to provide reliability backup for the other continuous subcarrier channels.

The system design objectives are to make precision measurements and to achieve maximum operational reliability. High stability, solid-state electronic regulators are incorporated in all power supplies. Critical voltage levels and operating temperatures are monitored. Of prime importance are the measurement of C_A and the radiometer in-flight calibration. Knowledge of C_A during flight is required to obtain accurate values of V_A. One-half of a full-scale model antenna was measured by the method of ground-plane imaging on an antenna test range to obtain the antenna capacitance and radiation characteristics prior to flight.

Utilization of the dummy antenna provides a simultaneous two-level calibration of all three radiometer channels. The radiometer zero-level response is obtained with no noise input; then a wide-band noise is introduced to determine the radiometer gain factors.

The pre-flight radiometer gain calibration with a temperature-limited diode was made with a balanced dummy antenna having an equivalent network (fig. 1) with C_A equal to the antenna free-space value. The resistance R_A is very small compared with the reactance of C_A, so the ratio of V_L, the voltage delivered to the receiver, to V_A is sensibly independent of the magnitude of R_A. It is therefore convenient to express the receiver output level in terms of the value of V_A^2 used in this calibration. Since noise is being measured the bandwidth may be neglected and the receiver output expressed in terms of the corresponding value of $T_A R_A$. The observational data will be expressed in these units. To obtain the true value of T_A in flight it is then necessary to correct the receiver output for the local value of C_A, and then to divide the resultant corrected value of $T_A R_A$ by the theoretical value of R_A. This is only valid if R_A is very small compared with the other impedances in the circuit, otherwise a more complicated analysis is necessary to obtain the true T_A.

All portions of this system functioned properly throughout the flight. A detailed technical description of the instrumentation will be published elsewhere.

4. Observational Data

A Journeyman four-stage solid-fuel rocket carrying the payload described above was launched by NASA from Wallops Island at 01:46 A.M. EST on 22 September 1962. An apogee of 1691 km was reached 798 sec after launch, with a sub-satellite point at latitude 39.32° N, longitude 66.40° W. Strong telemetry signals were received throughout the flight. Stations at Wallops Island and Bermuda jointly obtained telemetry reception until 1524 sec when the vehicle was below 50 km and presumably the performance was terminated by re-entry effects. The radio astronomy antennas were not fully extended until 233 sec at 725 km. The vehicle was in sunlight from 639 sec (1617 km on the upleg) to 1290 sec (965 km on the downleg). Analysis of the photocell data and of telemetry signal strength variations due to vehicle spin indicates that the vehicle had a spin period of 5.04 secs with no detectable precession. It is presumed that the spin axis was aligned with the velocity vector at burnout.

During the flight the ionospheric critical frequency was about 3 Mc. Aural and oscillographic inspection of the records of the unsmoothed audio outputs, which were sampled sequentially, indicated that with the receivers connected to the antenna there was no sign of anything other than pure noise in the receiver outputs from the time the antennas were fully extended until after 1490 sec. At the latter time, the vehicle was at about 200 km, well below the peak of the F-region, and voice and musical broadcast or impulsive interference was clearly audible on each receiver.

Data obtained on the bottomside of the ionosphere also indicated that the capacitance measurement was functioning correctly. The final reading obtained before the payload ceased to function, taken at about 75 km, was within less than 0.5 pf on the pre-flight ground measurement of 32 pf.

Fig. 6 gives a general impression of the radiometer and capacitance data throughout the flight. This is on a linear time scale and results in some distortion of altitude variations. Each point represents an average value for the sample of the relevant output taken during a 12-second sequence. The points have been joined by straight lines. This may give a somewhat false impression at times when rapid variations occur; occasionally a considerable increase or decrease is seen during a 6-second radiometer sample. Modulation at twice the spin frequency is seen on each

radiometer output throughout most of the flight. An averaged sample may not include an integral number of cycles, thus contributing to fluctuations on otherwise slowly varying portions of fig. 6. In general, the noise level on the radiometer outputs is below the level of these fluctuations.

Some of the important features of the data will be mentioned briefly. The 1.225 and 2.0 Mc radiometers show the general behavior expected about apogee, such as the outputs decreasing gradually with decreasing altitude. The antenna capacitance at apogee at 1.25 Mc is somewhat below its free-space value and falls off with decreasing altitude, also as expected. The 0.75 Mc radiometer output is fairly steady at a relatively low value for a wide range of altitude below 1600 km, but above this shows a rise which is rather abrupt in terms of altitude and apparently symmetrical about apogee.

At lower altitudes the data evidently becomes more complicated. The 2.0 Mc radiometer shows a rather abrupt fall below 600 km on the downleg, followed by a very sharp rise for a single 6-second sample, the increase being more than a factor of ten in one second before leveling off. By the next data sample, the 2.0 Mc output is negligible and stays so through the peak of the ionosphere. The 1.225 Mc output falls more gradually than the 2.0 Mc, flattens at about 1000 km, then rises rather rapidly to a level more than thirty times higher than its apogee value. It stays high for more than 200 km, then descends to a rather low value below 600 km altitude, and stays low through the peak of the ionosphere.

The capacitance on the downleg continues to fall until about 800 km, where it is somewhat less than half its free-space value. Then it rises rather rapidly until the measuring device saturates at about 75 pf, at which level it stays until below the peak of the ionosphere. No appreciable modulation of the capacitance which may be related to the spin period is observed, except possibly close to the minima and on the steep climb. Since the samples taken are discrete and within a 2-second interval, small amplitude modulation is not easy to detect, but a limit of perhaps 0.3 pf can be placed on these variations over most of the range.

On the upleg, the full sequence of events cannot be seen because the antenna was not fully extended until 725 km. There is a general similarity to the downleg phase although the behavior is not identical and is perhaps more complicated.

While the behavior of the 1.225 and 2.0 Mc radiometer outputs follows qualitatively the expected behavior for considerable distances either side of apogee, it would be imprudent to assume that this behavior is following its predicted theoretical course until the various other unexpected features can be explained. A desirable first step is a model of the ionospheric distribution over the trajectory.

5. The derived model ionosphere

It is tempting to assume that the rise in the 0.75 Mc radiometer close to apogee is due to the crossing of the line X = 1 on fig. 2, so that reception of the ordinary wave suddenly commences. This defines a point near apogee on the plasma frequency profile, and indicates, for example, that at 1.225 Mc reception of the extraordinary wave would barely commence before apogee. The decrease in the 1.225 Mc output is then due to the decrease in the ordinary wave portion of the radiation resistance, and an ionospheric profile can be constructed which will account for the general fall of the 2.0 and 1.225 Mc outputs. The sharp rises at 1.225 and 0.75 Mc at lower altitudes are likely to have a common though unknown cause because of the general similarity of their time duration and level.

At an early stage of the analysis, with limited samples of data reduced, this hypothesis was in fact adopted and preliminary estimates were made of cosmic noise intensities [21]. It seemed that the 2.0 Mc value deduced was fairly reliable because the corrections for plasma effects were small, though the 1.225 Mc value needed large corrections and was much less certain. As data reduction advance, however, this approach led to a number of problems which require a revised model of the ionospheric profile and therefore revised values of cosmic noise intensity at 1.225 Mc, but the 2.0 Mc measurement requires only a minor adjustment.

An important feature found in a detailed examination of the data is that the spin modulation of the 1.225 Mc radiometer output is strictly in phase with that of the 2.0 Mc above about 1050 km, and the two amplitudes of modulation are nearly equal at about $\pm$ 10 per cent of the respective mean levels, that at 1.225 Mc possibly being slightly greater; this is for more than half the time of flight. The 0.75 Mc spin modulation apparently bears no simple relationship to those at the other two frequencies in phase

or amplitude. This strongly suggests that the 2.0 Mc and 1.225 Mc modulations have a common source. It cannot be an anisotropic plasma effect since such an effect would be expected to be much more marked at the lower frequency (as may be checked numerically using the methods discussed in section 2), and to show some variation with altitude owing to changing plasma and gyro frequencies. The only remaining possible source of the modulation appears to be the antenna temperature T_A. As the vehicle spins, the gain distribution projected on the sky varies; map inspection of sky brightness distribution at higher frequencies suggest that the observed modulation is reasonable. Its phase, of course, would be expected to be random relative to any modulation due to the effect of magnetic field on C_A and R_A.

The conclusion that R_A is not appreciably modulated by spin enables an upper limit to be set to the plasma frequency at apogee. From inspection of the results of Weil and Walsh [17] (c.f. fig. 3) it is clear that it must be well below the critical frequency for the extraordinary wave given by X = 1-Y, i.e. in region 1 on fig. 2. Otherwise, the term N becomes quite large, and R_A is strongly dependent on angle relative to the magnetic field. Thus, as the vehicle descends, the extraordinary wave should disappear when it crosses the boundary into region 2 of fig. 2. This should be identifiable by several phenomena. From inspection of fig. 3 it is seen that there should be (i) a rather abrupt decrease in output, followed by a relatively slowly decreasing region, and (ii) a rapid change in the phase and perhaps modulation amplitude as the term N increases and R_A becomes angle-dependent.

At 1.225 Mc, it is found that the moderate rate of decrease becomes very rapid, the output falling by a factor of more than two in 20 seconds between 1247 sec (1089 km) and 1267 sec (1033 km), then flattening; in the same interval the phase changes after being stable for 15 minutes. This strongly suggests extraordinary wave disappearance between 1260 and 1265 sec. At 2 Mc the fall in output and change in phase are more spectacular suggesting extraordinary wave disappearance within 3 seconds of 1415 sec, though no flat region is seen after the disappearance.

Using these two rather closely defined points, a tentative topside ionospheric profile can be sketched using also the known ionosphere below the F-region peak. The latter is obtained from bottomside soundings at

Wallops Island. To take account of the fact that the vehicle is then displaced eastward from Wallops Island the soundings are taken at a local time approximately equal to that at the vehicle when descending through the peak of the ionosphere. Errors introduced here produce only a small effect on the topside profile. This data is, in fact, sufficient to define a reasonable profile up to about 1050 km (fig. 7). This, of course, has uncertainties, particularly at frequencies midway between the "anchor" points. Above the upper point the profile is derived from the measured capacitance data, using the approach due to Kaiser (discussed in section 2.3) but slightly modified to better fit a cylindrical geometry. A vehicle potential of the order -0.25 volts is expected and therefore an allowance is made for a corresponding sheath with a radius about 5 cm in the region above the upper point. The agreement at the point defined by the 1.225 Mc extraordinary wave disappearance is excellent. The profile above this point is not symmetrical about apogee and the curve shown in fig. 6 applies to the downleg path. This upper portion cannot be greatly in error. Final values of intensity are not critically dependent on its accuracy. The overall profile appears reasonable. Its general characteristics are consistent with current knowledge of the topside.

This provisional profile is then used to investigate quantatively the extraordinary wave disappearance. At 1.225 Mc a measured value of C_A is available and the mean value of R_A may be obtained from the results of Weil and Walsh [17]. The mean value of R_A is $M + N \langle \cos 2\phi \rangle$. The second term is known from the direction of the spin axis. Assuming constant T_A, the relative rate of decrease of the receiver output may be calculated during the presumed extraordinary wave disappearance. This is shown in fig. 8 together with the observed receiver output. The theoretical curve has been adjusted to give best fit around the cusp. The fit is strikingly good. After the disappearance, the theoretical curve, involving only the ordinary wave, falls away rather more rapidly than the observed points, but this is perhaps connected with the climb to the so-far unexplained high level which begins at 1320 sec. The modulation on the sample centered at 1257 sec apparently has the same phase the previous samples have shown since well before apogee, and the same phase as the 2.0 Mc modulation. However, by the next sample the phase has changed. From fig. 8 it seems that the identification of the extraordinary wave disappearance is quite

unambiguous. It is believed its time is accurate to less than ± 3 secr corresponding to about ± 10 km altitude, giving a very accurate point on the profile. A similar quantitative fit to the disappearance of the extraordinary wave at 2.0 Mc has been made.

6. Trajectories in the X-Y^2 plane

It is now of interest to investigate the trajectories of the three receiver frequencies on the X-Y^2 plane discussed previously, using the above model of the ionosphere. The trajectories after apogee are given in fig. 9. It will be shown that a number of features of the data summarized in section 4 now fall into a systematic pattern. The numbering of regions in fig. 2 will be used.

1.225 Mc enters region 3 at 1323 sec and leaves at 1410 sec. Because of the uncertainties in the profile the earlier time may be in error by as much as 10 sec, but the later one is probably rather accurate being close to the 2.0 Mc extraordinary wave disappearance. This interval is in remarkably close agreement with the period during which an apparently anomolous high output occurred.

2.0 Mc enters region 3 at 1429 sec and leaves at 1441 sec, these times probably being accurate to a few seconds. The only sample within this interval is the remarkable one described in section 4: the output rising very rapidly at 1432 sec from a low level, then returning to a low level before the next sample beginning at 1444 sec.

These facts suggest that 0.75 Mc be examined while in region 3. In fact, 0.75 Mc is in region 3 at apogee and passes out of it at 955 sec across the line Y = 1 (which is well defined from geomagnetic data independent of the model ionosphere). This coincides precisely with the disappearance of the high-level output around apogee, previously thought to be a cosmic noise received above the X = 1 level. Also, the increase commences precisely at the line Y = 1 before apogee.

It appears therefore that the sharp 2.0 Mc feature after extraordinary mode disappearance, the 1.225 Mc high-level noise also after extraordinary mode disappearance, and the 0.75 Mc rise around apogee should be classified together and attributed to the peculiar properties of region 3. Each is in this region of the X-Y^2 plane at different times,

at widely ranging altitudes, and for very different lengths of time, yet each shows an unexpectedly high level, falling again outside region 3. In addition, 2.0 and 1.225 Mc leave this region by crossing the line X = 1, while 0.75 Mc crosses the line Y = 1. This variety of conditions of of occurrence makes the identification with region 3 very strong. As pointed out in section 2, the theory of antenna behavior in this region appears to be poorly developed so it is perhaps not too surprising that unpredicted phenomena should occur. Cosmic noise can propagate into region 3 as wave I but not as wave II, and if the radiation resistance were high enough could produce a large antenna voltage, V_A. However, there is no reason to expect such behavior of the component I of R_A, and it seems that the effects observed in region 3 must be attributed somehow to wave II which has an infinity in the refractive index.

An obvious question then is the occurrence of a high output at 0.75 Mc overlapping in time the high level at 1.225 Mc and following a long period with a low output and little variation. 0.75 Mc enters region 7 at 1347 sec. This may be uncertain by up to 15 sec, but it coincides closely with the onset of the high level. 0.75 Mc crosses from region 7 to region 8 at 1410 sec, this time being accurate to a few seconds, but the level remains high for a considerably longer period. Again, in these regions antenna behavior is rather uncertain, this time because of the infinity in the refractive index of characteristic wave I. Tentatively, therefore, the feature on the 0.75 Mc output may be attributed somehow to the infinity of regions 7 and 8.

The origin of these unexpected noise levels in regions 3, 7 and 8 can only be speculated about on the basis of present data. It cannot be attributed to a thermal origin in the surrounding plasma because it can be shown, from knowledge of the receiver input impedance, that each case requires antenna temperatures of at least one to two orders of magnitude greater than the ambient temperature of the plasma, which is probably less than 1000°K. Antenna temperatures as low as this could only occur if the radiation resistance were several thousand ohms, to provide a power match to the receiver. It seems unlikely that such levels of radiation resistance occur, and if they were close to their free-space values, the antenna temperatures at 1.225 Mc in region 3 and 0.75 Mc in regions 7 and 8 would be

in excess of 10^8°K, and at 2.0 Mc and 0.75 Mc in region 3 about 10^6 and 10^7°K respectively.

A possible source is Cerenkov radiation from energetic charged particles. The requirement for a refractive index greater than unity is of course met in these regions.

7. Cosmic noise intensities

It now appears reasonably safe to assume that at the altitudes above the extraordinary wave disappearance levels at 1.225 and 2.0 Mc, the data may be used to obtain cosmic noise intensities. The radiometer outputs at apogee can be corrected using the measured C_A and the model ionosphere to obtain a value of T_A. Greater confidence in the answer would be generated, however, if consistency could be obtained in the corrected values at a number of points along the trajectory. Using the method outlined for 1.225 Mc in the previous section, a theoretical curve of the receiver output relative to its free-space value can be calculated. While measured C_A values are available for 1.225 Mc, it is necessary to compute them for 2.0 Mc; this again may be done using Kaiser's approach and assuming an appropriate sheath.

The comparison of the theoretical curves with the observations is made in fig. 10, where the theoretical curves have been placed to give best fit weighted toward apogee. It is seen that the fit at 1.225 Mc is extremely good; because the predicted curve is fitted to apogee rather than the extraordinary wave disappearance, the fit around the latter point is not quite as good as in fig. 8. At 2.0 Mc there is appreciable divergence around the shoulder before the rapid fall. However C_A at 2.0 Mc must be computed using the model ionosphere, and this divergence is greatest between about 1000 km and 600 km. This is the region between the two extraordinary wave disappearance points where, as pointed out previously, the model ionosphere is not too well-defined. Higher plasma frequencies would be required to make the theoretical curve fit the observed curve.

From fig. 10 the appropriate free-space value of $T_A R_A$, and hence of T_A, is determined. T_A is a non-uniformly weighted average of the sky brightness temperature in the upward hemisphere, which at apogee is centered on new galactic coordinates ℓ^{II}=144°, b^{II} = -19° or R.A. = 02:30, Dec.=39°.

The antenna is spinning about an axis which is nearly vertical. Since the zenith is the direction of maximum gain of the dipole antenna it is slightly more weighted than regions at low elevations. The excess gain produced by ionospheric focusing near the edge of the focused beam is very small in the case of a beam as broad as the one which applies around apogee. The difference between the value of T_A due to the true weighting function and a uniform one is probably very small.

The resulting average values of cosmic brightness temperature are given in table 2, together with the intensity, or brightness, defined by

$$I_\nu = 2kT_B \lambda^{-2} \quad .$$

No mention of the value at 0.75 Mc has been made. During the time in which 0.75 Mc is in region 6 of fig. 2, it should be receiving cosmic noise by the ordinary wave, so measurements of intensity should be possible. The radiometer output level is rather low in this region and careful attention must be paid to instrumental corrections. However antenna impedance should be predictable, and it may yet be possible to derive a useful estimate, if only an upper limit, of the intensity at 0.75 Mc. This will require much more analysis.

8. Spectrum of cosmic noise background

The mean cosmic noise intensity plotted against frequency is shown in fig. 11. The slope of a straight line spectrum on this graph is defined as the spectral index, X, such that mean intensity is proportional to $(\text{frequency})^X$. For comparison with the new 1.225 and 2.0 Mc points, higher frequency points, due to the Mullard Radio Astronomy Observatory [22-25], are selected as being probably the best values available in this frequency range. An attempt was made to adjust their intensity values to correspond to the mean intensity over the hemisphere observed at 1.225 and 2.0 Mc.

The points shown on the graph for Ellis et al [7] are minimum and maximum values observed in Tasmania and cannot easily be related to the reference hemisphere. This also applies to the value at 3.8 Mc by Chapman and Molozzi [10] which is included because it is the only other space radio astronomy value yet reported.

The intensity at 2.0 Mc taken in conjunction with the higher frequency intensities strongly suggests a straight line spectrum with index near -0.5. These data exclude a spectral index steeper than -0.6, such as recently used by Hoyle and Ellis [26], and they exclude an index flatter than -0.4. They also appear to exclude any sensible break in the slope of the intrinsic cosmic noise spectrum above 10 Mc, as reported by Turtle et al [24].

The fact that the intensity at 1.225 Mc is one-half the value at 2 Mc indicates that interstellar absorption by ionized hydrogen must be invoked to account for this rapid intensity decrease. A change in intrinsic spectrum due to synchrotron self-absorption is unlikely at so high a frequency. Nor is a change of the intrinsic synchrotron spectrum due to the onset of energy losses of the cosmic ray electrons by ionization of interstellar matter adequate to account for such a sudden drop-off.

9. Radio emission from the artificial radiation belt of 9 July 1962

On 9 July 1962 the U. S. exploded a high altitude hydrogen bomb which injected relativistic electrons into the trapped orbits, thereby creating an artificial radiation belt. These trapped electrons emitted synchrotron radiation which was observed by ground-based telescopes at frequencies between 18 and 100 Mc. This emission has been discussed by Nakada [27]. Before the rocket experiment on 22 September 1962 the authors considered the possibility that synchrotron radiation from this artificial radiation belt would interfere with the rocket measurements of cosmic noise. Since the radiation from the artificial belt was localized over the geomagnetic equator and the rocket shot was to be made at a magnetic latitude +52°, the fraction of the total sky filled by the artificial belt was quite small and it was decided to proceed with the rocket experiment. This decision has since been justified by the studies of Nakada made after the rocket shot. Nakada has kindly carried out machine calculations of the intensity of 1 Mc radiation on 22 September 1962 viewed from apogee of the rocket trajectory. By neglecting ionospheric refraction and assuming that the antenna pattern was isotropic, he obtained a value of 5.4×10^6°K. Using the spectrum given by Nakada for the synchrotron radiation from the artificial belt viewed from the geomagnetic equator, we extrapolate from this value at 1 Mc to obtain 1.2×10^6 °K at 2.0 Mc, 3.4×10^6 °K at 1.225 Mc and 10^7 °K at 0.75 Mc. The corresponding intensity values are 1.47,

1.56, 1.72 in units of 10^{-21} W $m^{-2}(c/s)^{-1}$ sr^{-1}. These values are several times below the observed intensities at 1.225 and 2.0 Mc; the contribution to the 2.0 Mc value is less than 8 per cent. No further consideration will be given to the artificial radiation belt since its contribution is expected to be less than the absolute accuracy of final intensity values, and the observed spin modulation of T_A at 1.225 and 2.0 Mc is not in phase with that expected from the radiation belt.

Conclusions

The mean intensity of the cosmic noise background over a celestial hemisphere away from the galactic center was measured at 1.225 and 2.0 Mc. The corresponding intensities are 1.0×10^{-20} and 2.0×10^{-20} W $m^{-2}(c/s)^{-1}$ sr^{-1}, with an estimated uncertainty of $\pm$ 1.5 decibel and the corresponding radio brightness temperatures are 2.1×10^{7} °K and 1.7×10^{7} °K at 1.225 and 2.0 Mc, respectively. The 2.0 Mc intensity combined with selected high frequency values referred to the same celestial hemisphere indicates a spectral index for the galaxy of approximately -0.5.

The drop of intensity between 1.225 and 2.0 Mc cannot be accounted for by ionization losses by the cosmic ray electrons or by synchrotron self-absorption, but requires free-free thermal absorption.

Intense noise signals were detected and the conditions for their occurrence were identified with propagation characteristics in the ionosphere at the three frequencies.

The effects of the anisotropic plasma on the radiation resistance of the radio astronomy antenna were detected. Variations in the radiation resistance during the onset of the disappearance of the extraordinary wave were identified.

It was demonstrated that the antenna behavior in the ionosphere is predictable and can be corrected to obtain cosmic noise intensity values outside the regions where the index of refraction may be infinite.

No interference from signals generated below the F-layer peak were detected.

TABLE I

Payload switching sequence

Time	Function	Radio Astronomy Antenna Connection	C_A Measurement Status	Preamp Connection	Noise Generator Status
0-6 sec.	Cosmic Noise Measurement	To Preamp	Off	To RA Antenna	Off
6-8 sec.	Radiometer Base-Line Calibration	To C_A Circuit	Off	To Dummy Antenna	Off
8-10 sec.	Radiometer Gain Calibration	To C_A Circuit	Off	To Dummy Antenna	On
10-12 sec.	Antenna Capacitance Measurement	To C_A Circuit	On	To Dummy Antenna	On

TABLE II

Cosmic Noise Intensities

Frequency (Mc)	Cosmic Brightness Temperature (°K)	Intensity ($W\ m^{-2}(c/s)^{-1}sr^{-1}$)
1.225	2.1×10^{7}	1.0×10^{-20}
2.0	1.7×10^{7}	2.0×10^{-20}

Acknowledgement

The authors wish to express their thanks to the National Aeronautical and Space Administration for financial support, and to the many individuals at the Goddard Space Flight Center and the Wallops firing range who prepared the rocket and conducted the launch. In particular, we owe thanks to Charles Campbell, John Guidotti and Lloyd Lohr. We appreciate the reduction of ionograms for the period of launch by the National Bureau of Standards. We are grateful for the assistance of James Kuiper, Hal Estry and Richard Miller in the design, test, and launching of the payload and data reduction, and John Dickel in the telemetry system design. We thank Mrs. Abigail Beutler for assistance on the data analysis, and Newbern Smith for constructing model ionospheres for aid in planning and analysis. Finally, we wish to thank E. H. Vestine of Rand Corporation for supplying geomagnetic data along the flight path, and M. P. Nakada of NASA for calculations of radio emission from the July 9, 1962 artificial radiation belt.

References

1. G. G. Getmantsev, V. L. Ginzburg and I. S. Shklovskii, UFN 66 (1958) p. 157
2. F. T. Haddock, Amer. Rocket Soc. 794 (1959) pp. 602-794
3. A. C. B. Lovell, Proc. Roy. Soc.A. 253(1959) p. 494
4. E. A. Benediktov, G. G. Getmantsev and V. L. Ginzburg, Iskusstvennye Sputniki Zemli, 7 (1961) p. 3. Trans. by R. Matthews, Planet. Space Sci. 9 (1962) pp. 109-127
5. G. Reber and G. R. Ellis, J. Geo. Res. 61 (1956) pp. 1-10
6. G. R. Ellis, J. Geo. Res. 62 (1957) pp. 229-234
7. G.R.A.Ellis, M. D. Waterworth and M. Bessell, Nature 196 (1962) p. 1079
8. J. P. I. Tyas, C. A. Franklin and A. R. Molozzi, Nature (1959) p. 184, p. 785
9. A. R. Molozzi, C. A. Franklin and J. P. I. Tyas, Nature 190 (1961) pp. 616-617
10. J. H. Chapman and A. R. Molozzi, Nature 191 (1961) p. 480
11. J. H. Chapman, Effects of the Ionosphere on Radio Noise Measurements from an Earth Satellite, Space Res. II, Proc. 2nd Internat. Space Science Symp. (1961)
12. F. G. Smith, Nature 191 (1961) p. 1381
13. D. Walsh, Ionospheric Focussing, Abstracts of the URSI Meeting (May 1961)
14. C. B. Haselgrove, Jenifer Haselgrove and R. C. Jennison, Proc. Roy. Soc. A. 261 (1961) pp. 423-434 (corrigendum Proc. Roy. Soc. A. 261 (1961))
15. F. G. Smith, Mon. Not., Roy. Ast. Soc. 122 (1961) pp. 527-534

16. H. Kogelnik, J. Res. N. B. S. 64D (1960) pp. 515-523

17. H. Weil and D. Walsh, Radiation Resistance of an Electric Dipole in a Magneto-Ionic Medium, PTGAP Intern. Symp. (1963) (to be published)

18. J. A. Ratcliffe, The Magneto-Ionic Theory and Its Applications to the Ionosphere, Cambridge Univ. Press, Great Britain, (1959)

19. T. R. Kaiser, Planet. Space Sci. 9 (1962) pp. 639-657

20. J. A. Kane, J. E. Jackson and H. A. Whale, J. Res. N. B. S. 66D (1962) pp. 641-648

21. F. T. Haddock, H. F. Schulte and D. Walsh, Ast. J. 68 (1963) p. 75

22. J. E. Baldwin, Mon. Not., Roy. Ast. Soc. 115 (1955) pp. 684-689

23. I. I. K. Pauliny-Toth and J. R. Shakeshaft, Mon. Not., Roy. Ast. Soc. 124 (1962) pp. 61-77

24. A. J. Turtle, J. F. Pugh, S. Kenderdine and I. I. K. Pauliny-Toth, Mon. Not., Roy. Ast. Soc. 124 (1962) pp. 297-312

25. A. J. Turtle and J. E. Baldwin, Mon. Not., Roy. Ast. Soc. 124 (1962) pp. 459-476

26. F. Hoyle and G. R. A. Ellis, Austr. J. Phys. 16 (1963) (in press)

27. M. P. Nakada, Synchrotron Radiation Calculations for the Artificial Radiation Belt, JGR (submitted)

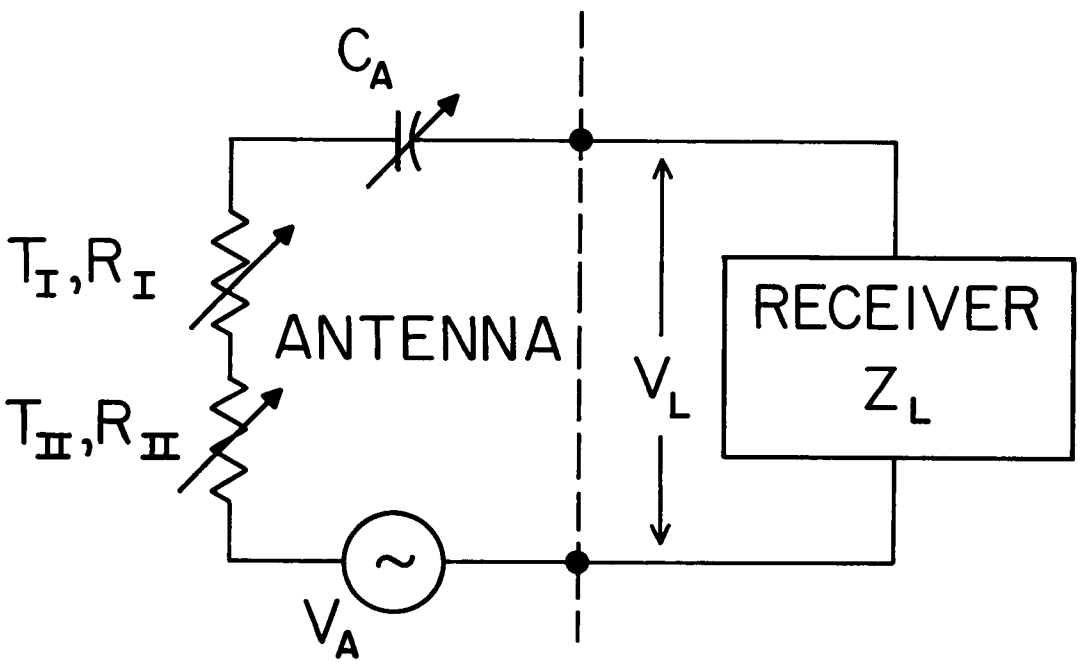

I. EQUIVALENT CIRCUIT OF ANTENNA AND RECEIVER INPUT NETWORK

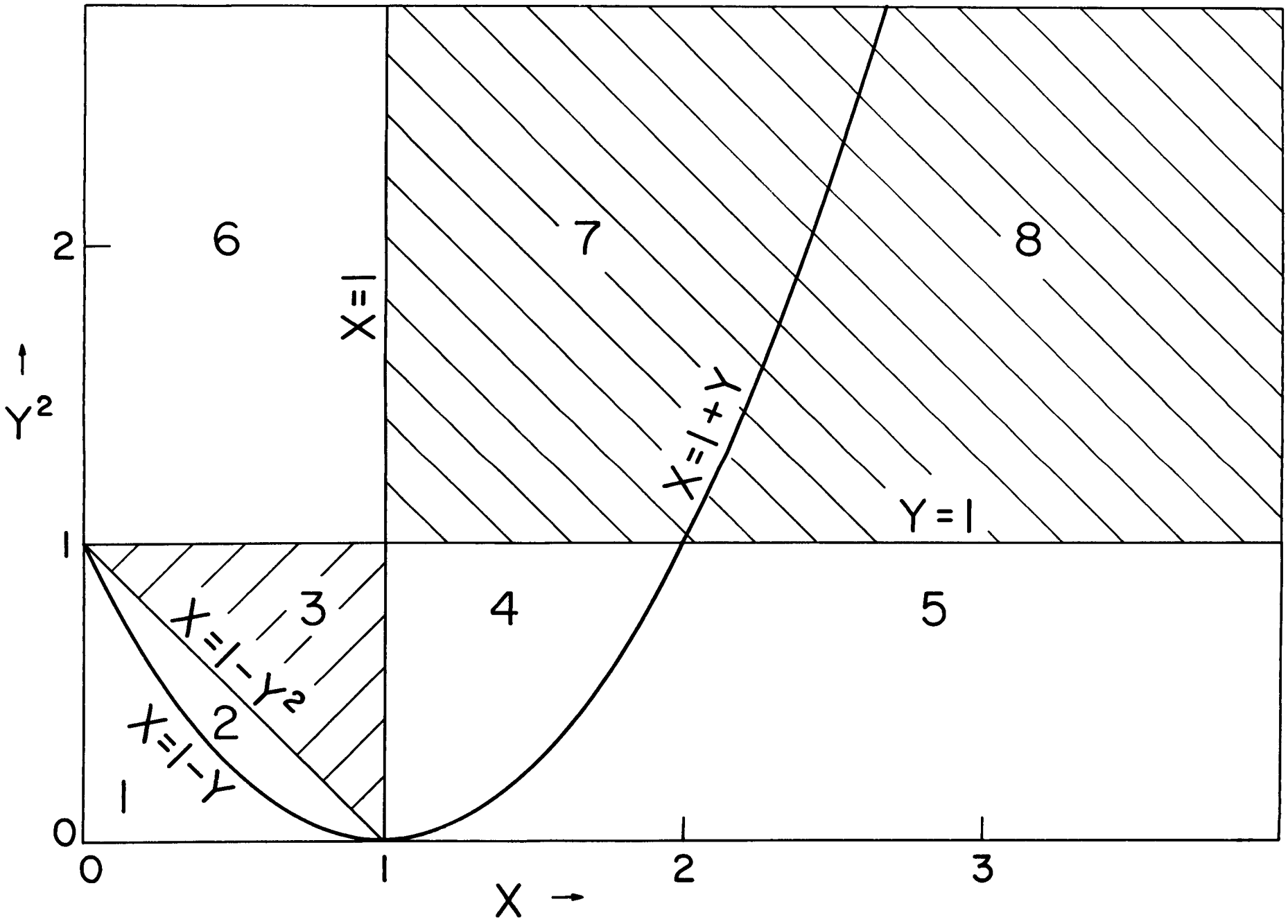

2. THE $X - Y^2$ PLANE

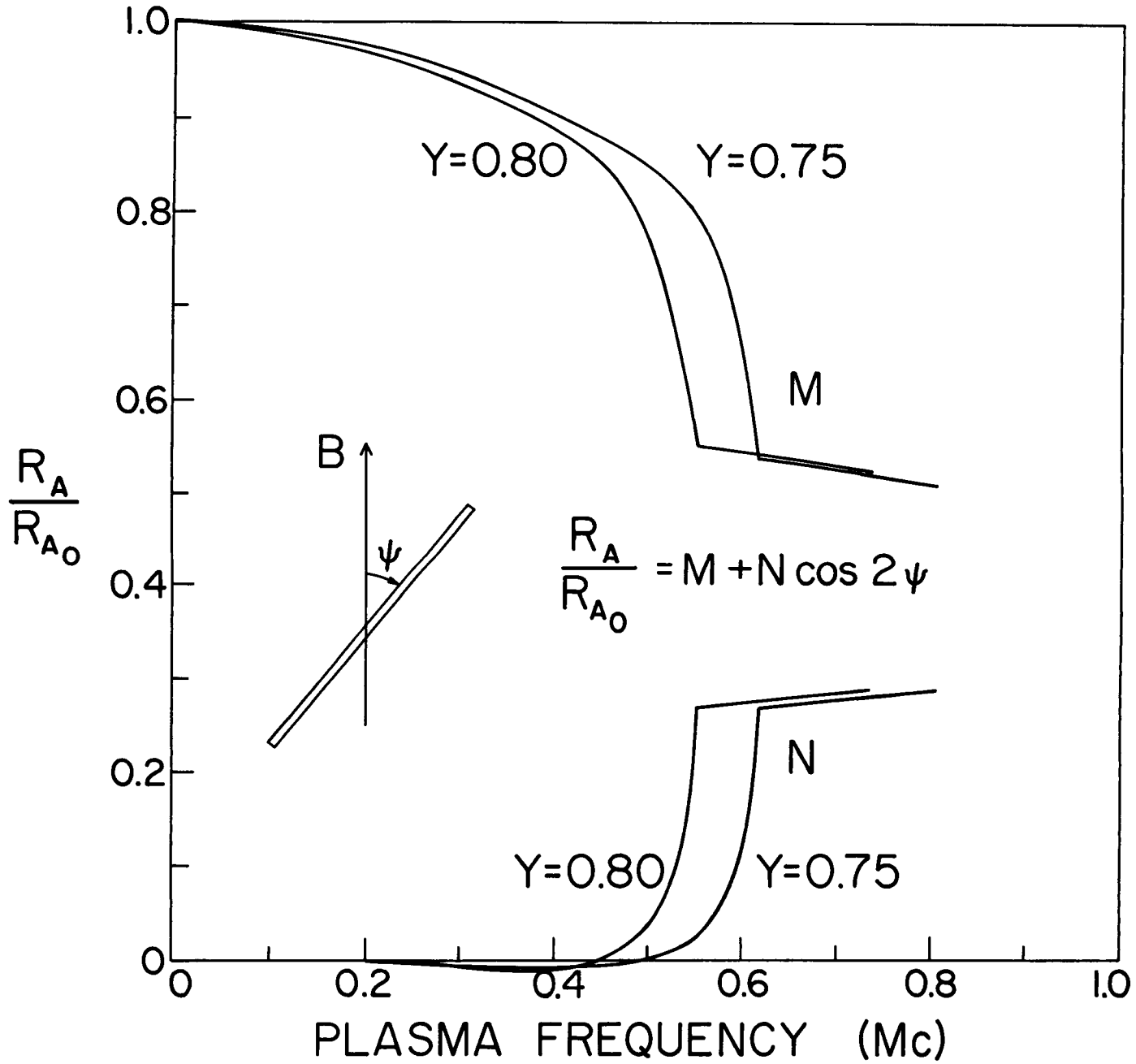

3. RELATIVE RADIATION RESISTANCE AT 1.225 Mc AS A FUNCTION OF PLASMA FREQUENCY FOR SELECTED VALUES OF Y

UNIV. OF MICH. - RADIO ASTRONOMY OBSERVATORY

COSMIC NOISE ROCKET MEASUREMENT

22 SEPT 62 NASA ROCKET 11.02 UR

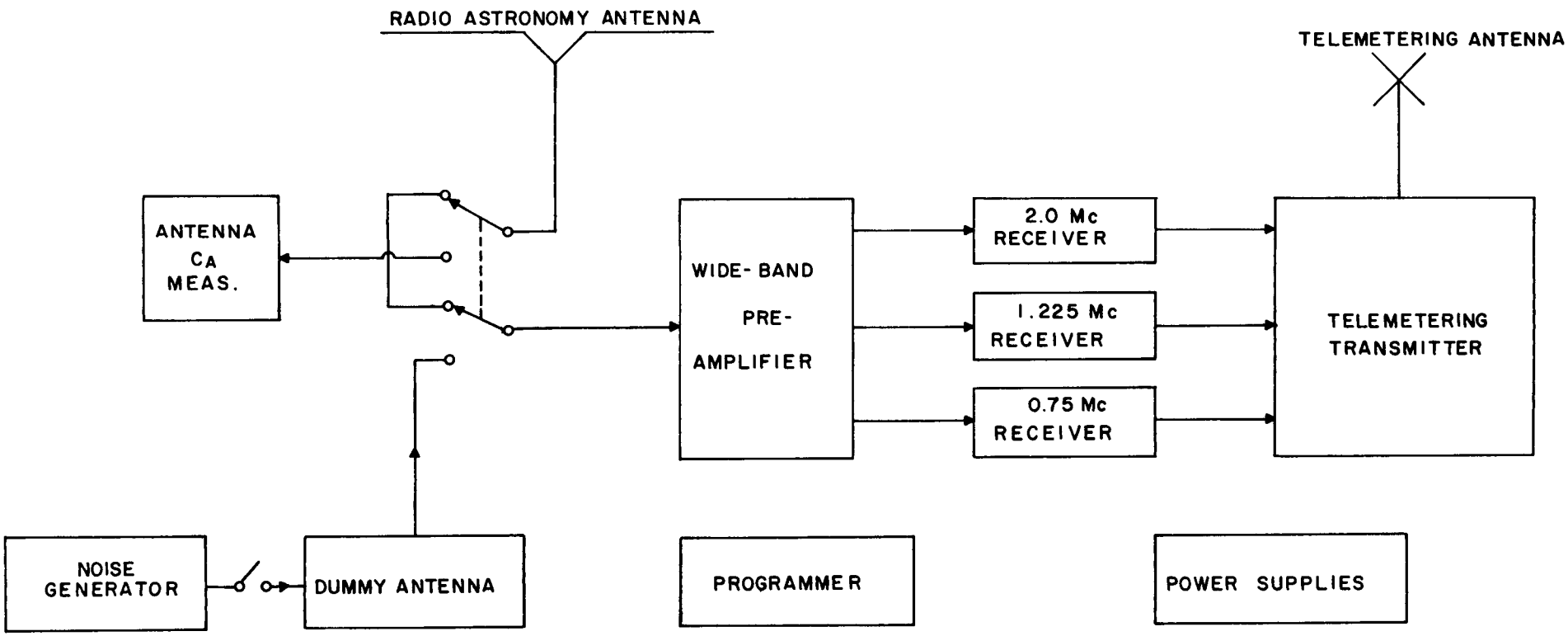

4. SIMPLIFIED SYSTEM DIAGRAM

UNIV. OF MICH. - RADIO ASTRONOMY OBSERVATORY

COSMIC NOISE ROCKET MEASUREMENT

22 SEPT 62 NASA ROCKET 11.02UR

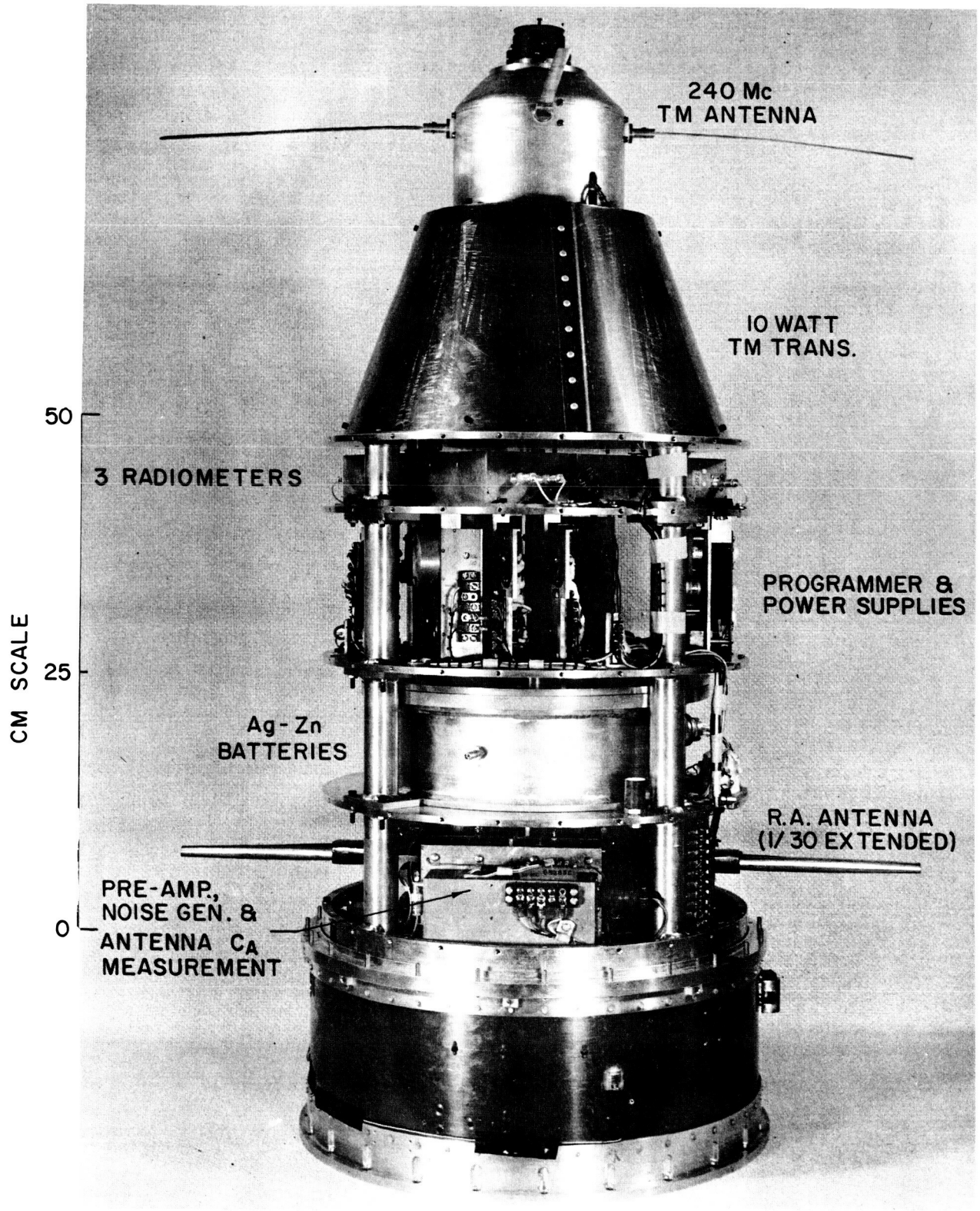

5. PAYLOAD, EX. SKIN & NOSE CONE

WT = 98 LBS.

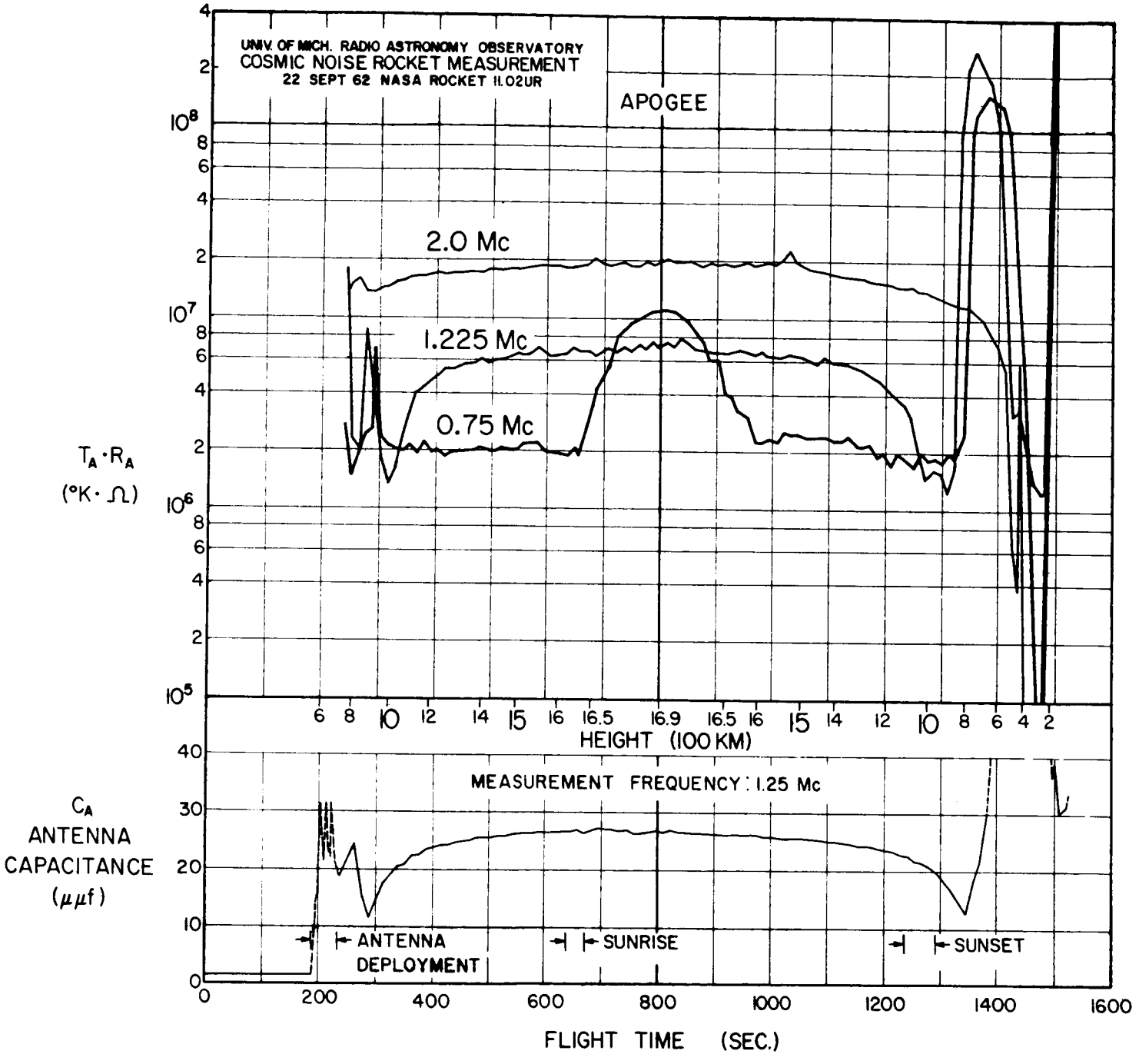

6. RADIOMETER OUTPUTS & ANTENNA CAPACITY RESULTS DURING FLIGHT

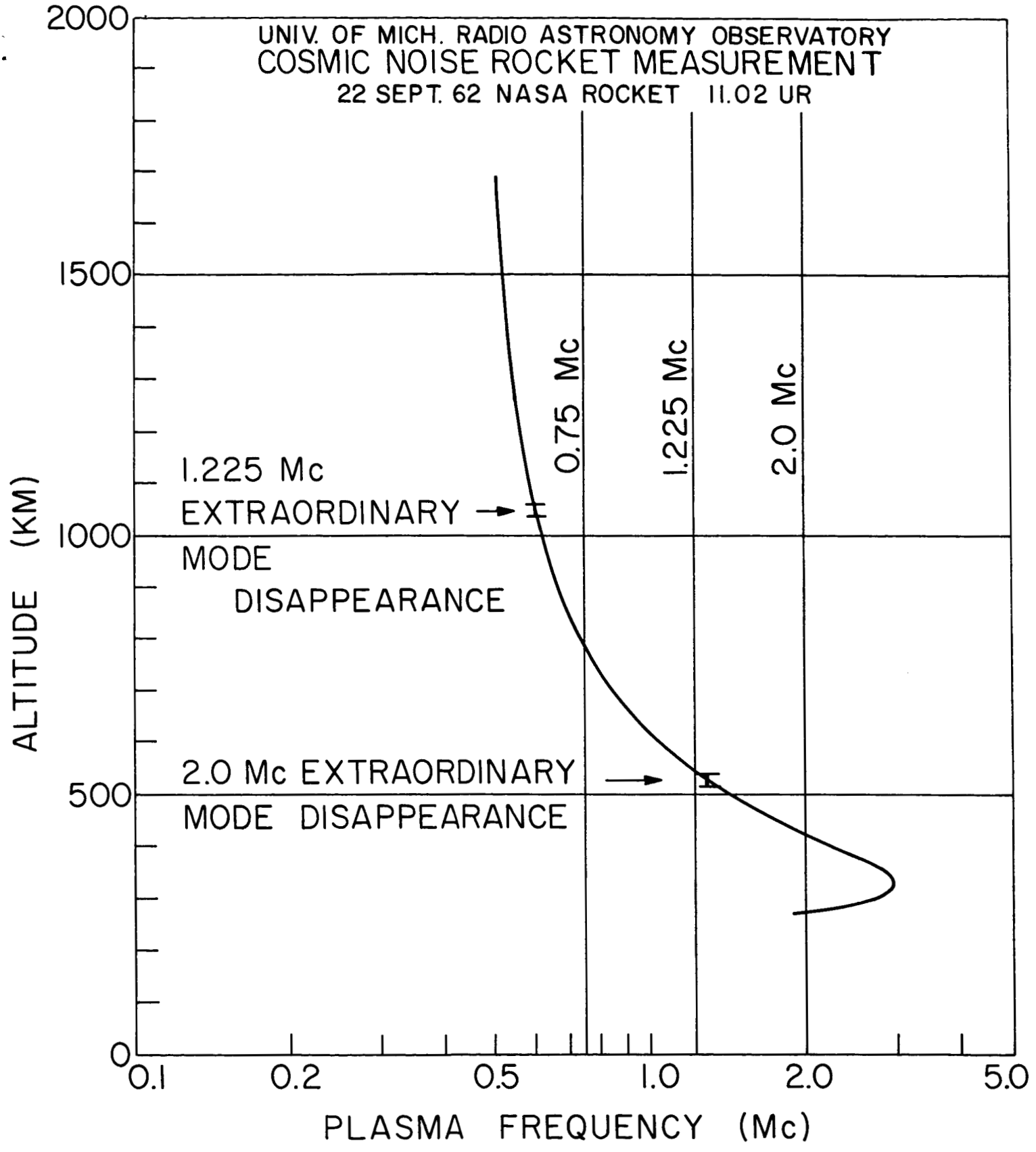

7. MODEL IONOSPHERE DEDUCED FROM FLIGHT DATA AND IONOSONDE

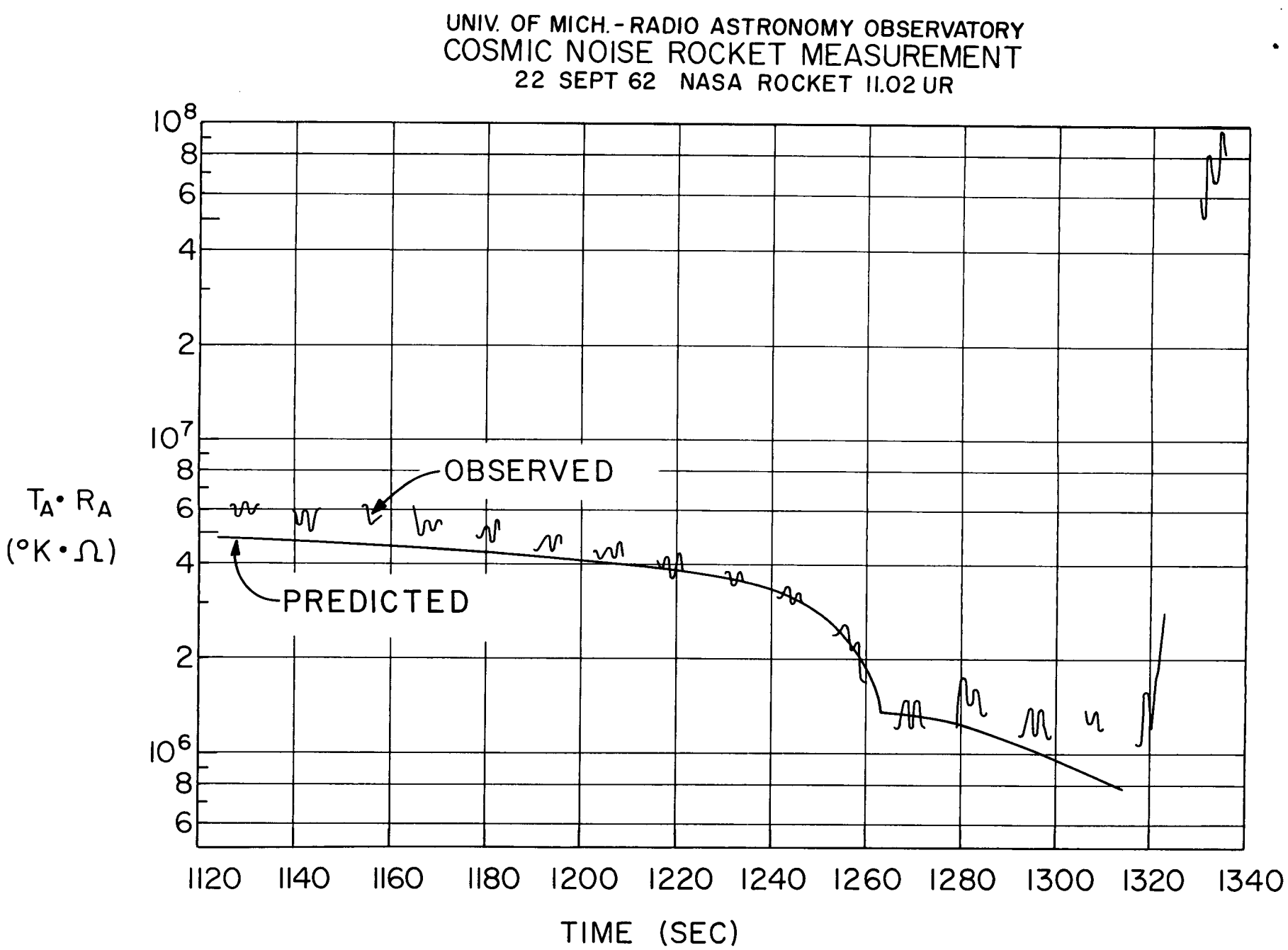

8. COMPARISON OF 1.225 Mc RADIOMETER OUTPUT WITH THEORETICAL CURVE FROM MODEL IONOSPHERE DURING EXTRAORDINARY WAVE DISAPPEARANCE

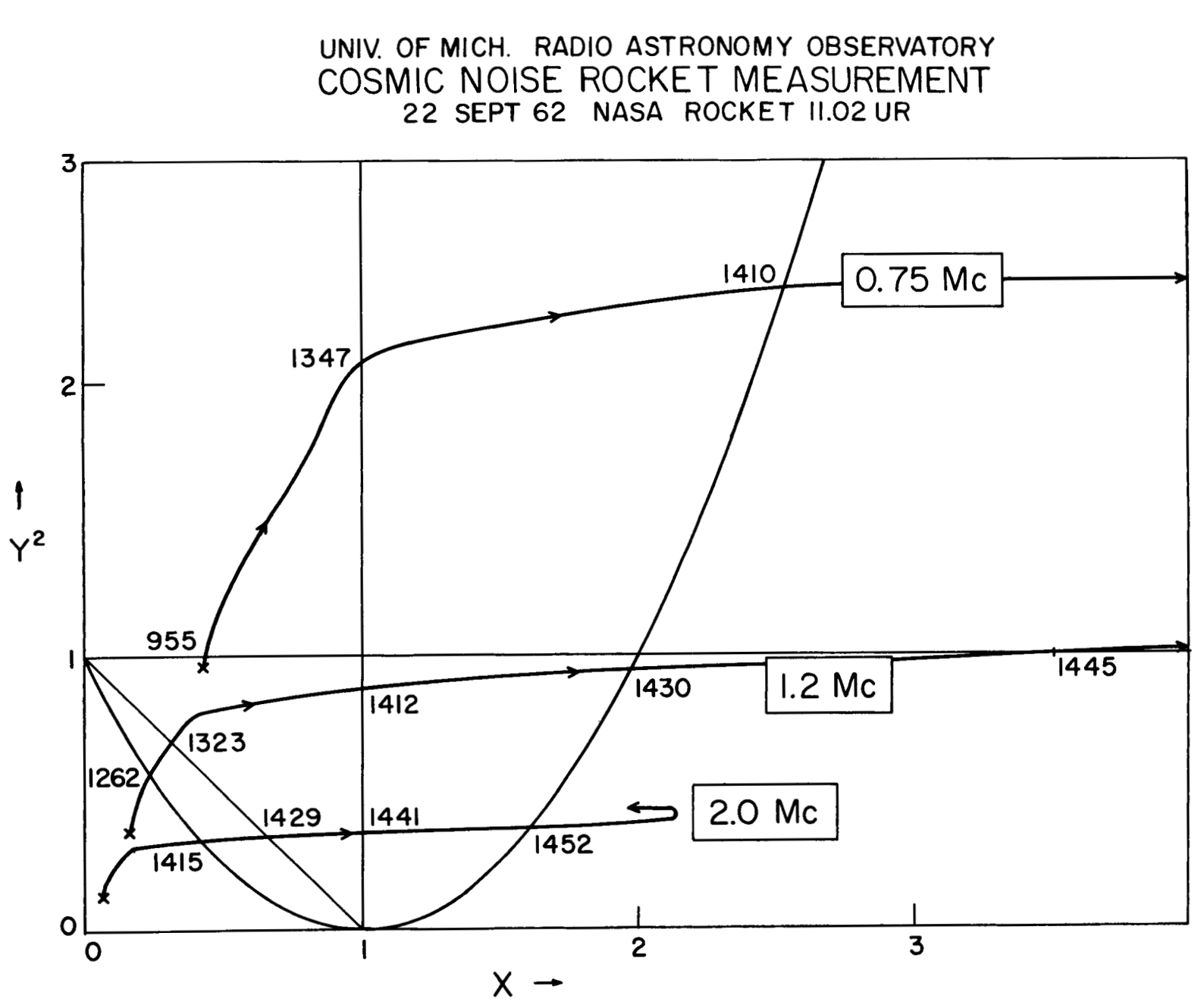

9. TRAJECTORIES OF RADIOMETER FREQUENCIES ON $X-Y^2$ PLANE. FLIGHT TIMES (IN SECS) MARKED AT REGION BOUNDARIES.

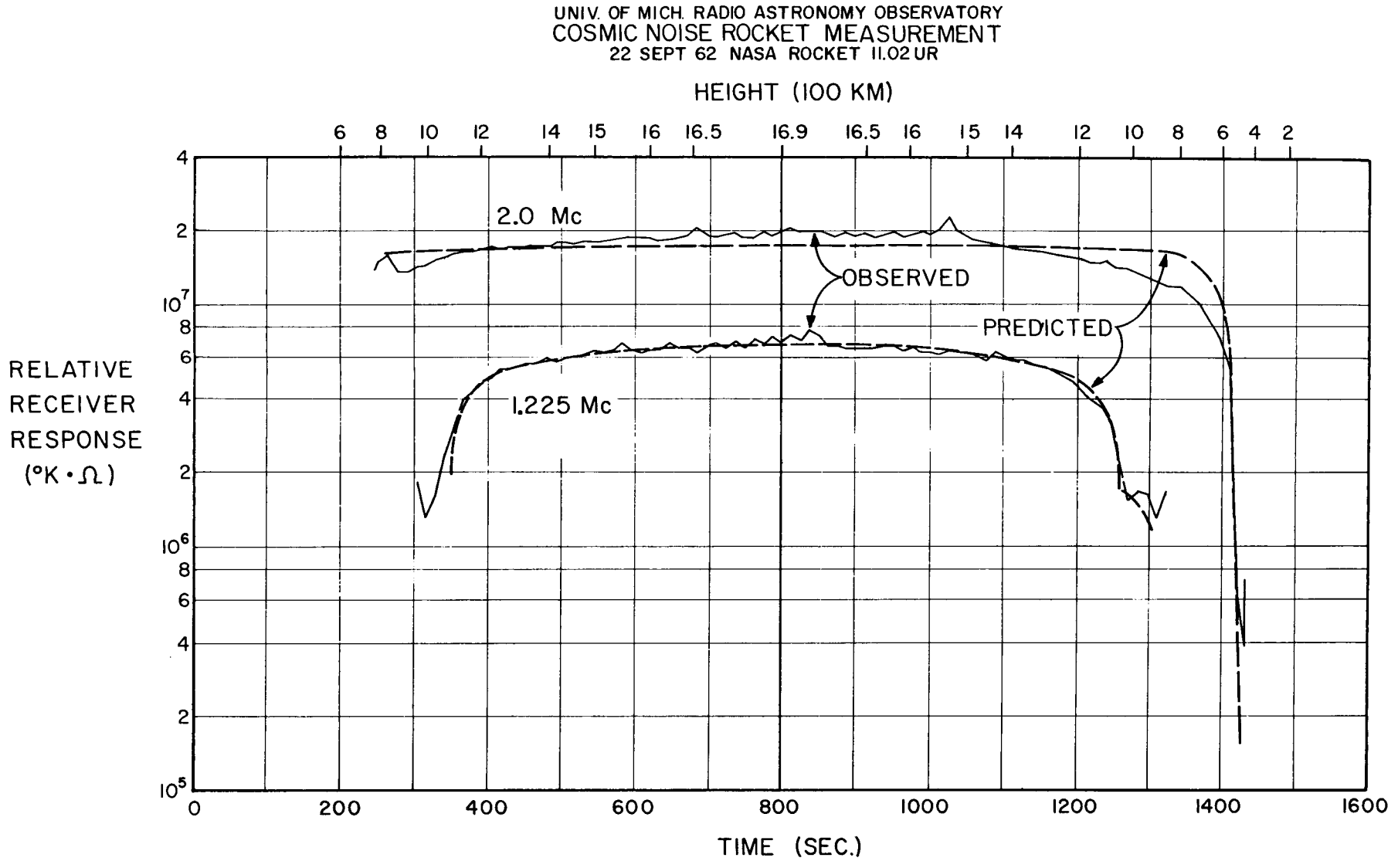

10. OBSERVED OUTPUTS COMPARED WITH PREDICTED RELATIVE RESPONSES

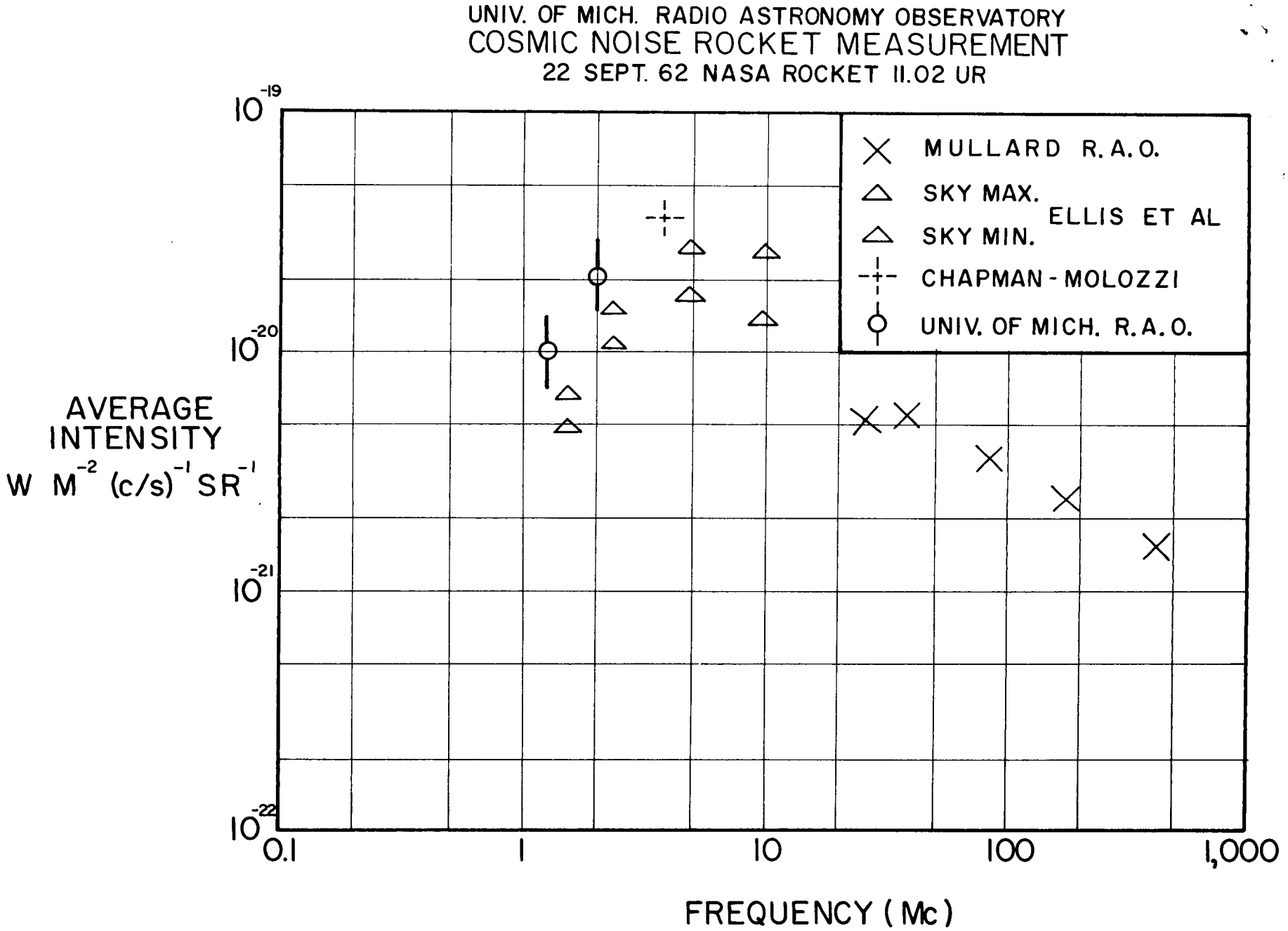

11. AVERAGE COSMIC NOISE SPECTRUM IN OBSERVED HEMISPHERE WITH SELECTED HIGHER FREQUENCY VALUES